Int. J. Nano Dimens., 9 (2): 158-169, Spring 2018

ORIGINAL ARTICLE

Route of administration induced in vivo effects and toxicity responses of Zinc Oxide nanorods at molecular and genetic levels

Sangeetha Aula[1,2]; Samyuktha Lakkireddy[1,2]; Atya Kapley[1,3]; Vedanta Narasimhaswamy Adimadhyam[4]; Rakesh Kumar Sharma[5]; Shantveer G Uppin[6]; Kaiser Jamil[1*]

[1]Centre for Biotechnology and Bioinformatics, Jawaharlal Nehru Institute of Advanced Studies (JNIAS), Secunderabad, Telangana, India

[2]Department of Biotechnology, Jawaharlal Nehru Technological University Anantapur (JNTUA), Ananthapuramu, Andhra Pradesh, India

[3]Environmental Genomics Division, Council of Scientific and Industrial Research- National Environmental Engineering Research Institute (CSIR-NEERI), Nagpur, Maharashtra, India

[4]Department of Chemical Engineering, Jawaharlal Nehru Technological University Anantapur (JNTUA), Ananthapuramu, Andhra Pradesh, India

[5]Division of CBRN Defence, Institute of Nuclear Medicine and Allied Sciences (INMAS), Delhi, India

[6]Department of Pathology, Nizam's Institute of Medical Sciences (NIMS), Hyderabad, Telangana, India

Received 05 October 2017; revised 08 January 2018; accepted 18 January 2018; available online 03 February 2018

Abstract

Zinc oxide (ZnO) nanoparticles have received growing attention for several biomedical applications. Nanoparticles proposed for these applications possess the potential to interact with biological components such as the blood, cells/ tissues following their administration into the body. Hence we carried out in vivo investigations in Swiss Albino Mice to understand the interaction of ZnO nanorods with the biological components following intravenous and oral routes of administration to assess nanoparticles safety. Intravenously injected ZnO nanorods were found to induce the significant reduction in the red blood cells and platelet counts. Elevated levels of serum enzymes such as serum glutamate oxaloacetate transaminase, serum glutamate pyruvate transaminase were observed following intravenous and oral administration. Also, increased levels ($p<0.05$) of oxidative stress markers such as glutathione in the liver of intravenous treated mice and liver, spleen of oral treated mice; and lipid peroxidation in the spleen of intravenous treated mice compared to untreated mice. Significant DNA damage was observed in liver, spleen, and kidney of mice treated intravenously; liver and kidney of mice treated orally compared to untreated mice. Histology revealed focal venous congestion in the liver of intravenous and oral treated mice; more red pulp congestion in the spleen of oral treated mice compared to the intravenous treated group; pulmonary vascular congestion in intravenous (mild) and oral treated mice (moderate). In conclusion differences in the histology of the organs tested could be due to the differences in the distributed concentrations of nanoparticles. These findings can be considered helpful for the development of biocompatible nanoparticles for biomedical applications.

Keywords: *Genotoxicity; Hemocompatibility; Histopathology; Oxidative stress; Zinc oxide nanoparticles.*

How to cite this article

Aula S, Lakkireddy S, Kapley A, AVN S, Kumar Sharma R, G Uppin Sh, Jamil K. Route of administration induced in vivo effects and toxicity responses of Zinc Oxide nanorods at molecular and genetic levels. Int. J. Nano Dimens., 2018; 9 (2): 158-169.

INTRODUCTION

In recent years, significant advancements in the field of biomedical nanotechnology resulted in the development of various revolutionary clinically viable products, which is evident from the variety of nanotechnology based products commercialized, and in use in clinical and preclinical studies [1-4].

For disease therapy and imaging applications, nanoparticles are usually administered by intravenous (i.v.) or by oral routes. After i.v. administration, the nanoparticles encounter and interact with systemic circulation and may further interact with blood components and subsequently distribute to various tissues of the body [5] where

* Corresponding Author Email: kaiserjamilgene@gmail.com

these may interact with the tissue components including cells. Therefore, understanding of the biological interactions and the toxicological properties of the nanoparticles proposed for an intended biomedical application is crucial even if the nanoparticles show excellent efficacy/ performance.

Among the different types of nanoparticles, inorganic ZnO nanoparticles have received greater attention for diverse biomedical applications such as disease therapy (as drug delivery vehicles and/ or therapeutic agents), imaging, tissue engineering etc. For instance, ZnO nanoparticles have been used as efficient drug delivery devices for sustained release of Daunorubicin, an anticancer drug used in the treatment of leukemia, wherein the cytotoxic effect of Daunorubicin administered as nanoparticle formulation was found enhanced under UV irradiation [6, 7] suggesting the potential application of ZnO nanoparticles in drug delivery. The ZnO nanoparticles were also employed for modulating allergic reactions in rat mast cell line RBL2H3, wherein increasing intracellular Zn^{2+} concentrations led to a decreased FcεRI-mediated mast cell degranulation through inhibition of the activities of PI3K (Phosphatidylinositide-3-kinase) and protein tyrosine kinase [8]. Similarly, ZnO nanoparticles effectively ameliorated the mast cell-mediated allergic inflammatory reaction in phorbol-12-myristate 13-acetate plus calcium ionophore A23187 (PMACI)-stimulated human mast cell line (HMC-1) [9], suggesting the application of ZnO nanoparticles as potential therapeutic agents for the treatment of mast cell-mediated allergic diseases.

In addition to the above applications, luminescent ZnO nanoparticles were employed for cell imaging [10]. Luminescent ZnO nanoparticles have also been employed in the detection of metal ions such as copper (Cu^{2+}) [11] and cobalt (Co^{2+}) [12], organic molecules such as dopamine (DA) [13], picric acid (PA) [14], and bisphenol A (BPA) [15] and proteins such as carbohydrate antigen 19-9 (CA 19-9) [16] in the biological system. Detection of such ions, organic molecules, and biomolecules by the luminescent nanoparticles is based on the quenching of their luminescence which enables the early diagnosis of various diseases, neurological disorders and cancers, thus ZnO nanoparticles have been considered as promising candidates for bioimaging applications.

In tissue engineering, ZnO nanoparticles loaded scaffolds were used to induce the upregulation of key angiogenic factors such as fibroblast growth factor (FGF), vascular endothelial growth factor (VEGF) (Augustine *et al.*, 2014) [17].

On the other hand, the potential of ZnO nanoparticles in inducing membrane injury, inflammatory response, DNA damage and apoptosis in mammalian cells [18-21] has also been reported. Moreover, most of these studies were carried out with in vitro systems that lack the complex cell–cell and cell–matrix interactions unlike in vivo [22]. Although some in vivo studies revealed the absorption, biodistribution and excretion profile of ZnO nanoparticles (Cho *et al.*, 2013; Lee *et al.*, 2012; Baek *et al.,* 2012) [23-25] which showed that ZnO nanoparticles are majorly distributed to liver, kidneys, lungs, and spleen and the resultant damage to the organs such as liver and lung [22, 26-28], a systematic assessment of nanoparticles interaction with key components (blood, cells/ tissues) to evaluate their toxicological properties are limited. Moreover, ZnO nanoparticles are of toxicological interest not only due to their medical uses but also because their non-engineered counterpart constitutes one of the most important components of workplace air pollution in copper and copper alloys smelters [29].

In our previous report (Aula *et al.*, 2014) [30], we found that the ZnO nanorods showed comparatively higher toxicity than the nanospheres. Thus in the present study, we have investigated the in vivo effects administered as acute doses to mice by intravenous or by oral routes and assessing the hematological, serum biochemical parameters and histopathology. The in vivo genotoxic effects of these nanoparticles in selected tissues have also been assessed. To understand the mechanism of cell death induced by ZnO nanorods, the oxidative damage by glutathione (GSH) estimation and lipid peroxidation (LPO) has been studied. These investigations are considered to provide important information on the influence of administration route on the ZnO nanorods biodistribution and also on the toxicological properties of these nanoparticles in vivo.

EXPERIMENTAL

Materials

Normal melting agarose (NMA), Ethylene diaminetetraacetic acid (EDTA) disodium salt, sodium lauroyl sarcosinate were purchased from

Sigma Aldrich Corporation (St. Louis, MO 63103, USA). Ultra-low gelling agarose was obtained from BDH Electra, BDH laboratory supplies (Poole, England; 44415 2G). Propidium iodide (PI) and 4', 6-diamidino-2-phenylindole (DAPI) were procured from Sigma Aldrich Chemicals Pvt Ltd (Bangalore, Karnataka, India). Boric acid was purchased from Glaxo Laboratories Ltd (Mumbai, Maharashtra, India). Phosphate buffered saline (Ca^{2+}, Mg^{2+} free PBS), Trypan blue, 2-Thiobarbituric acid (TBA), Trichloroacetic acid (TCA), Ellman's reagent (DTNB reagent-5, 5'-Dithiobis(2-Nitro Benzoic Acid) were obtained from Himedia Pvt Ltd (Mumbai, Maharashtra, India). All other chemicals were obtained of analytical reagent grade.

Methods

Preparation and Physicochemical characterization of ZnO nanorods aqueous dispersion

ZnO nanorods powder was a kind gift from Centre for Nanomaterials, International Advanced Research Centre for Powder Metallurgy and New Materials (ARCI), Hyderabad. ZnO nanorods dispersion was obtained by the addition of nanorods powder to the milli-Q water, under stirring, to obtain a concentration of 100 µg/ml (stock). Prior to use for the experiments, the stock suspension was vortexed, sonicated using a probe sonicator at 34 W 40% amplitude for 10 min, vortexed again to obtain a uniform suspension. The physicochemical characterization such as X-ray diffraction (XRD) and specific surface area (SSA) of ZnO nanorods were reported previously (Aula *et al.*, 2014). The morphology, diameter, length distributions etc of ZnO nanorods were determined from images obtained by field emission scanning electron microscopy (FESEM, S-4300-SE/N, Hitachi, Japan).

Animals and Treatment

All animal handling procedures were carried out as per the regulations of Institutional Animal Ethics Committee (IAEC), Institute of Nuclear Medicine and Allied Sciences (INMAS), Delhi with their prior approval for using the animals. Male Swiss Albino Mice (~6-weeks old, 27 ± 3 g) were obtained from INMAS central animal facility and were housed in a 12 h day and light cycle environment with the availability of diet and water, at the controlled temperature of 23 ± 2 °C, humidity of 55 ± 5%. Animals were acclimatized to this environment for 7 days prior to the experiment and were fasted overnight before treatment.

The animals were divided into 3 groups containing 3 animals each: Group 1-Control or untreated (administered water); Group 2- ZnO nanorods (2.4 mg/kg body weight) administered intravenously; Group 3- ZnO nanorods (2.4 mg/kg body weight) administered orally. Selection of nanorods dose for the proposed study is based on the maximum dispersibility of nanorods in milli-Q water and maximum injected volume of nanosuspension into mice. After the treatments for 3 days, animals were anesthetized with inhaled methoxyflurane (Penthrane, Abbott Laboratories, UK), blood was collected by cardiac puncture for hematology and serum biochemistry assays and the organs were collected immediately for isolation of single cells and also for histopathology studies.

Hematology and Serum Biochemical assays

The whole blood collected from three groups of mice were mixed with disodium EDTA and were analyzed for hematological parameters such as Red blood cell (RBC) count, Hemoglobin (Hgb), Hematocrit (HCT), Mean corpuscular volume (MCV), Mean corpuscular Hgb (MCH), Mean corpuscular Hgb concentration (MCHC), Red cell distribution width (RDW), White blood cell (WBC) count, Platelet count, Mean platelet volume (MPV), Plateletcrit (PCT) using Automated hematology analyzer (CELLTAC α NIHON KOHDEN, MEK-6450K, Japan). The serum was obtained by centrifugation of whole blood at 2500 rpm for 15 min. The serum biochemical levels such as serum glutamate oxaloacetate transaminase (SGOT), serum glutamate pyruvate transaminase (SGPT), creatinine, bilirubin and urea were assayed by a fully Automated Biochemistry analyzer (Roche, Hitachi 902, Manheim, Germany). Standard controls were run before each assay.

Oxidative stress

- Total Glutathione measurement

Total glutathione content in the tissues of liver, spleen, and kidney of mice treated intravenously and orally with ZnO nanorods was measured as described by Beutler 1963 [31]. A 10% (W/V) homogenate of tissues were prepared in 0.1 M ice cold PBS (pH 7.4) by homogenization using hand-held homogenizer (IKA T10, Germany). Tissue homogenates were centrifuged in a refrigerated centrifuge (Combi 514R, Hanil, South Korea) at

8,000xg for 10 min at 4 °C. The supernatants obtained were treated with precipitating reagent (in 1 : 2 ratio) containing metaphosphoric acid, disodium EDTA, and NaCl centrifuged for 10 min at 2500xg. The supernatant obtained was used for analysis. 200 µL of supernatant was mixed with 650 µL of disodium hydrogen phosphate (Na_2HPO_4) buffer (0.3M) and 150 µL of Ellman's reagent and measured the absorbance of yellow color at 412 nm. Blank without sample was prepared similarly and absorbance was recorded at 412 nm. Total protein content in the supernatants obtained by centrifugation of tissue homogenates was estimated by Bradford's method. Total GSH content was expressed as µmoles of GSH/mg protein.

- Lipid Peroxidation assay

LPO content in the tissue homogenates of liver, spleen, and kidney (see Total Glutathione measurement section for preparation of tissue homogenates) of mice treated intravenously and orally with ZnO nanorods was measured using the thiobarbituric acid method as described by Laughton *et al.*, 1989 [32]. Briefly, 600 µl of tissue homogenates were incubated with 100 µl of TCA (10% W/V) at 37 °C for 1 h and then centrifuged at 1000xg (Combi 514R, Hanil, S Korea) for 10 min at room temperature. To the supernatant, 100 µl of TBA (0.67% W/V in 0.025 M NaOH) was added and incubated at 80 °C for 30 min. The absorbance of pink coloured TBA-Malondialdehyde (MDA) complex developed was measured at 535 nm using Gen5 software (Powerwave XS2, Biotek, USA). The extent of LPO was expressed as µmoles of MDA/mg protein.

Genotoxicity

- Single cell gel electrophoresis assay (Comet assay)

Liver, spleen, and kidney tissues of mice treated intravenously and orally with ZnO nanorods were minced and single cell suspension was prepared in 0.1M chilled PBS. Cell viability assessment was made for all the experiments of comet assay as per the guidelines of Tice *et al.,* 2000 [33]. Cells isolated from all the organs were diluted with PBS and viability was checked with 0.4% trypan blue dye. The viable cells with intact cell membrane excluded the dye and were counted using hemocytometer under inverted phase contrast microscope (CKX 31, Olympus Corporation, Japan). Neutral Comet assay was performed as described previously by Khaitan *et al.*, 2006 [34]. Briefly the cell suspension containing approximately 10,000 cells mixed with 0.75% ultra-low gelling agarose was layered onto microscopic slides precoated with 0.1% NMA and incubated at 4 °C for 10 min. Lysis was performed by placing the slides in neutral lysis buffer (2.5% SDS, 1% Sodium lauroyl sarcosinate, 25 mM EDTA; pH 9.5) for 15 min at 25-30°C. Slides were then washed in distilled water for 5 min and electrophoresis was performed at 2 V/cm (400 mA) for 5 min at 10 °C in electrophoresis buffer (90 mM Tris base, 90 mM Boric acid, 2.5 mM EDTA; pH 8.4). Slides were rinsed again in distilled water for 5 min, air dried at 45°C on a hot plate and stored in a cool humid box until use. Following rehydration in distilled water, comets were stained with PI (50 µg/ml in PBS) and images were acquired in fluorescence microscope (BX60, Olympus, Japan) with appropriate fluorescence filter (WG; Olympus) using FA87 monochrome CCD camera (Grunding, Germany) and Optimas Image Analysis Software (Optimas USA; version 5.2). The comet parameters such as olive tail moment (OTM) and %Tail DNA were used to measure DNA damage in the cells. Analysis of DNA distribution in the comets was performed using Komet 5.5 software, Kinetic Imaging, USA.

- Micronuclei (MN) assay

MN formation in the liver, spleen, and kidney tissues of mice untreated and treated intravenously and orally with ZnO nanorods was assessed as described previously (Khaitan *et al.*, 2006) [34]. Air-dried slides containing methanol-acetic acid (3 : 1 V/V) fixed cells of the tissues were stained with a DNA specific fluorochrome DAPI (3 µg/ml). Slides were then examined under the fluorescence microscope using UV excitation filter and fluorescing nuclei were visualized under blue emission filter. Cells containing micronuclei were counted from >1000 binucleated cells by employing the criteria of Countryman and Heddle 1976 [35]. The fraction of cells containing micronuclei (%M-fraction) was calculated as follows:

%M-fraction= N_m/N_t X100, where N_m is the number of cells with micronuclei and N_t is the total number of cells analyzed.

Histopathological studies

The organs (Liver, spleen, kidney, and lung) isolated from untreated and ZnO nanorods

treated mice were fixed in 10% formalin for 48 h at room temperature. Dehydration of tissues using different concentrations of alcohol (70%, 80%, 95% and 100%) and subsequent clearing of the dehydrating agent by xylene were performed using Automatic Tissue Processor (Spencers, Model No. 1040-STP-004). The dehydrated tissues were then embedded in paraffin blocks in Tissue Embedding System (Spencers, Model No. 3080-STE-004), which were then sliced into 5 µm in thickness under microtome and placed onto clean glass slides. Following hematoxylin-eosin (H&E) staining, the slides were examined by light microscopy for histopathological changes.

Statistical analysis

Data represent mean and standard error mean (mean ± SEM) of three biological replicates from each group of experimental mice. The data were analyzed by means of one way analysis of variance (ANOVA) with Dunnett's test wherever applicable to determine the significant difference between treated and untreated using Graph pad prism 6.05 (Graph Pad Software, Inc., La Jolla, CA, USA). $P < 0.05$ was considered statistically significant in all the cases.

RESULTS AND DISCUSSIONS

The increasing application of ZnO nanoparticles for biomedical use such as disease therapy, imaging, etc requires a thorough knowledge of their interaction with various biological components, consequences of those interactions, mechanisms associated with the toxicity aspects from molecular biology and genetic standpoints to assess nanoparticles safety.

In our previous study, we had assessed the biological interactions in vitro of ZnO nanorods with human peripheral lymphocytes and found that these nanorods induced excess formation of reactive oxygen species (ROS) led to oxidative stress mediated DNA damage, reduction in RBC and platelet count (Aula *et al.,* 2014) [30]. In the present study, the acute toxicity of ZnO nanorods in mice was investigated after an exposure of 3 days and measured the hematological and serum biochemical parameters, oxidative stress, DNA damage and histopathological effects.

Physicochemical characterization of ZnO nanorods

FESEM studies revealed the rod shaped morphology of ZnO nanoparticles (Fig. 1). These nanorods possess 30-250 nm length.

Hematology and serum biochemical assays

Hematological parameters in the blood of mice treated intravenously and orally with ZnO nanorods were determined by automated hematology analyzer and listed in Table 1. Significant reduction in RBC and platelet count was observed in mice treated intravenously with ZnO nanorods compared to that of the untreated group. Reduction in the RBC counts suggesting possible induction of anemia whereas the reduction in the platelet counts suggesting thrombocytopenia. This may lead to disturbances in the homeostasis and undesired platelet aggregation may lead to blockage of blood vessels. Biochemical parameters in the serum were detected by autoanalyzer and are listed in Table 2. The significant increase in SGOT and SGPT levels in mice administered intravenously and orally with ZnO nanorods compared to that of the untreated group was observed. Significantly increased SGPT levels were observed in i.v. treated mice compared to oral treated mice whereas significantly increased SGOT levels were observed in oral treated mice compared to i.v. treated mice. The increased levels of serum enzymes indicated the effect of ZnO nanorods treatment in inducing liver injury similar to that observed by Esmaeillou *et al.*, 2013 [26].

Oxidative stress

The potential of ZnO nanorods in inducing oxidative stress was assessed by measuring the oxidative stress markers such as GSH and LPO levels in the treated and untreated groups and are shown in Figs. 2(a, b). A significant increase in GSH levels was observed in the liver of mice treated intravenously and orally with ZnO nanorods compared to untreated. GSH levels were slightly, but not significantly, increased in the spleen of mice treated intravenously, whereas, significantly increased in oral treated mice compared to untreated. In the kidney of intravenously treated mice, GSH levels were faintly increased compared to untreated, whereas the significant difference was observed between GSH levels of the kidney of mice treated intravenously and orally with ZnO nanorods (Fig. 2a). LPO levels were not significantly altered in the liver of intravenous and oral treated mice compared to untreated. In the spleen of intravenous treated mice, LPO levels were significantly increased compared to untreated. LPO levels were slightly increased in the kidney

Table 1: Hematology of mice treated intravenously and orally with ZnO nanorods.

Name of the parameter	Control	ZnO nanorods i.v.	ZnO nanorods Oral
WBC ($x10^3$/µl)	4.50±0.34	4.00±0.75	4.33±0.37
RBC ($x10^6$/µl)	8.85±0.57	7.06±0.2[a]	7.7±0.57
Hgb (g/dL)	13.6±0.57	12.5±1.15	12±1.15
HCT%	42.5±4.04	39.3±5.19	38±2.88
MCV (fL)	48.0±5.19	49.6±5.77	50.1±2.88
MCH (pg)	15.4±1.15	15.8±1.73	14±1.73
MCHC (g/dL)	35.3±1.76	32.1±3.17	30±2.88
PLT ($x10^3$/µl)	742±34	621±11[a]	676±23
LY%	71.3±5.77	79.9±7.5	72±7.5
GR%	28.7±2.3	20.1±2.3	28±2.88
RDW%	16.6±1.73	14.7±1.73	13.8±1.15
PCT%	0.26±0.03	0.23±0.02	0.2±0.02
MPV (fL)	3.5±0.28	3.4±0.28	3.4±0.23
PDW%	20.4±2.88	20.4±3.46	17.1±0.57

[a]Significant difference ($p<0.05$) compared to control;
[b]Significant difference ($p<0.05$) between i.v. and oral treatments.

Table 2 : Serum biochemistry of mice treated intravenously and orally with ZnO nanorods.

Name of the parameter	Control	ZnO nanorods i.v.	ZnO nanorods Oral
SGOT (IU/L)	83.0±4.04	101±5.19[a]	139±5.77[a,b]
SGPT (IU/L)	25±3.46	74±5.19[a,b]	51±5.19[a]
Urea (mg/dL)	53±7.5	55±4.6	55±5.77
Creatinine (mg/dL)	0.15±0.02	0.12±0.04	0.25±0.02
Total bilirubin (mg/dL)	0.35±0.04	0.35±0.02	0.25±0.04

[a]Significant difference ($p<0.05$) compared to control;
[b]Significant difference ($p<0.05$) between i.v. and oral treatments.

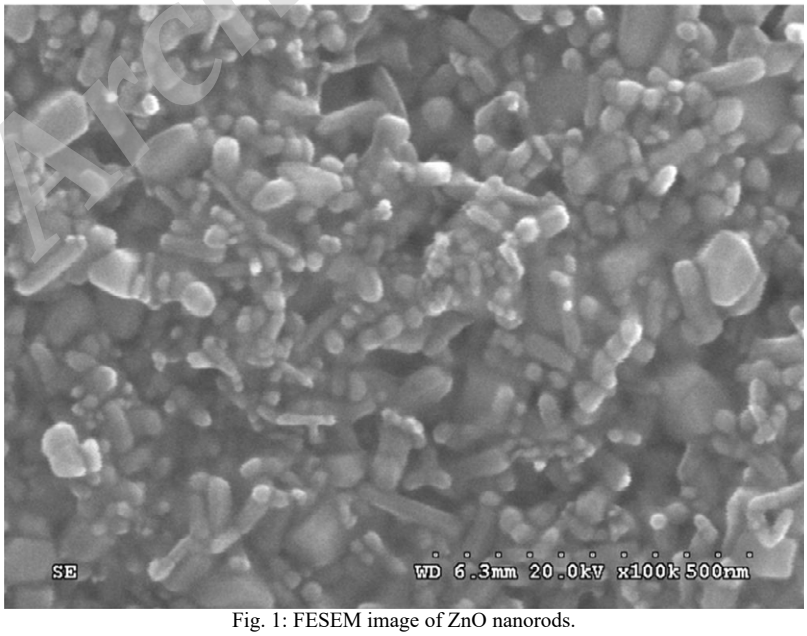

Fig. 1: FESEM image of ZnO nanorods.

of oral treated mice compared to untreated and intravenous treated mice (Fig. 2b). The increased GSH levels thus neutralize the effects of ROS in liver of mice treated intravenously and orally, but these levels were thought to be insufficient to neutralize the effects of excess formed ROS in the spleen of mice treated intravenously with ZnO nanorods and hence induced LPO which is evident from the increased LPO levels. LPO further induce the generation free radicals which can subsequently damage biomolecules such as DNA, lipids, and proteins.

Genotoxicity

Oxidative DNA damage in the liver, spleen, and kidney cells of mice treated intravenously and orally with ZnO nanorods was evaluated using neutral comet assay. Cell viability was found to be greater than 90% for all the samples. A statistically significant DNA damage in the liver, spleen, and kidney tissues of mice treated intravenously and liver, and kidney tissues of mice administered orally was observed which was evident by the significant increase in OTM and %Tail DNA compared to control. DNA damage was significantly higher in the liver and kidney tissues of oral treated mice than that of intravenous treated and in the spleen of intravenous treated than oral administered (Table 3). DNA damage in the form of comets is shown in Fig. 3 (a, b, c; a1, b1, c1; a2, b2, c2). MN formation was significantly increased in liver and spleen of mice treated intravenously with ZnO

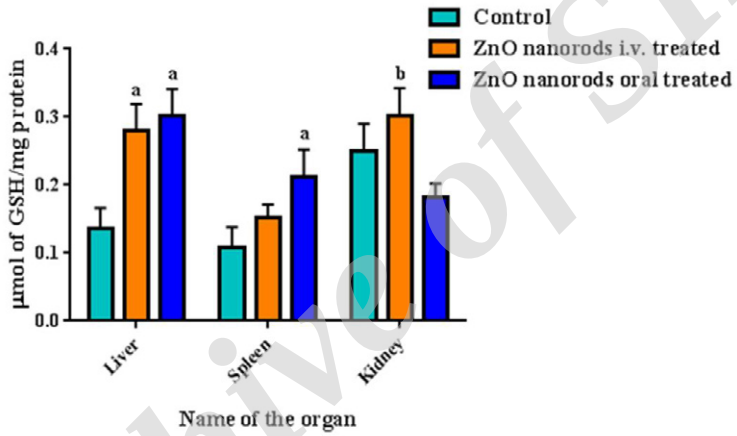

2(a)

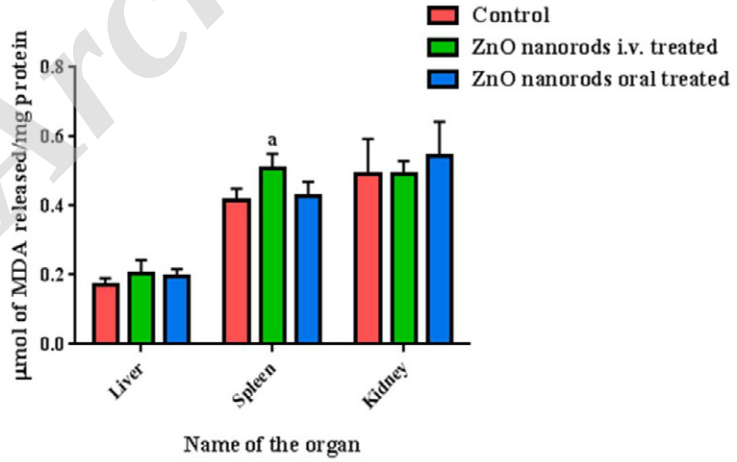

2(b)

Fig. 2: Quantification of (a) GSH (b) LPO levels in liver, spleen and kidney tissues of mice treated intravenously and orally with ZnO nanorods. asignificant ($p < 0.05$) difference compared to control; bsignificant ($p < 0.05$) difference between intravenous and oral treatments. i.v.- intravenous.

nanorods compared to control while the increase was marginal in case of the kidney. ZnO nanorods induced the significant increase in MN formation in the liver while the increase was marginal in case of spleen and kidney of mice following oral administration compared to untreated. Noteworthy i.v. the route led to significantly increased MN formation in the spleen compared to oral route (Table 4). Genotoxic potential of ZnO nanorods treatment following i.v. and oral routes measured by two different methods i.e., comet assay and MN formation assay displayed the similar pattern of toxicity in the organs tested.

DNA damage observed in liver, spleen, and kidney of mice treated intravenously and liver and kidney of mice treated orally with ZnO nanorods could be potentially due to either (i) the direct interaction of nanorods with cellular DNA and/ or (ii) the interaction of higher concentrations of LPO products resulted from nanorods treatment (as these also evident from the increased LPO products as discussed in oxidative stress section). Higher DNA damage observed in liver and kidney of mice treated orally with ZnO nanorods than intravenously treated and spleen of intravenously treated than the oral might be due to the higher absorption and distribution of nanorods to these tissues. In general, i.v. the route may be expected to higher exposure of nanoparticles to the tissues, but in our case lack of pharmacokinetic data of these two different routes of administration didn't allow understanding of the reasons for differences in exposures of the nanoparticles after two different routes of administration and make links between exposure and toxicity.

Histopathology studies

Histological alterations of liver, spleen, lung and kidney tissues of mice treated intravenously and orally with ZnO nanorods were observed under the light microscope following H&E staining. Liver of mice administered intravenously and orally with ZnO nanorods showed focal venous congestion (portal and central vein) (Figs. 4a,4b,4c,4d,4e,4f). This may be due to the accumulation of nanorods in these veins, leading to congestion, which may result in liver damage as evident from increased SGOT and SGPT levels, DNA damage, MN formation. Due to congestion in the portal vein (a condition known as portal vein thrombosis-blockage or narrowing of the portal vein), blood cannot flow properly through the liver may lead to portal hypertension and cause potential problems with the liver function. Congestion in the central vein leads to the development of pressure in it, which may lead to a condition known as "passive hepatic congestion" and may cause elevations in the liver enzymes such as SGOT, SGPT (Alvarez and Mukherjee., 2011) [36].

Spleen of mice administered orally with ZnO

Table 3 : Comet parameters of liver, spleen and kidney of mice treated intravenously and orally with ZnO nanorods.

S.No.	Name of the sample	Olive tail moment			%Tail DNA		
		Liver	Spleen	Kidney	Liver	Spleen	Kidney
1	Control	1.28 ±0.06	2.34 ±0.04	1.99±0.017	11.68 ±0.75	20.68 ±1.12	22.51 ±0.61
2	ZnO nanorods i.v.	3.00 ±0.1[a]	3.97 ±0.08[a,b]	2.70 ±0.04[a]	30.17 ±1.1[a]	30.85 ±0.88[a,b]	22.27 ±0.43
3	ZnO nanorods oral	3.91 ±0.07[a,b]	2.62 ±0.04	4.49 ±0.09[a,b]	27.3 ±0.46[a]	20.25 ±0.48	30.8 ±0.58[a,b]

aSignificant difference ($p<0.05$) compared to control; bSignificant difference ($p<0.05$) between i.v. and oral treatments.

Table 4 : %M-fraction of liver, spleen and kidney of mice treated intravenously and orally with ZnO nanorods.

S.No.	Name of the sample	Micronuclei (%)±SEM		
		Liver	Spleen	Kidney
1	Control	0.7±0.11	1.3±0.17	1.7±0.4
2	ZnO nanorods i.v.	3.0±0.17[a]	4.1±0.4[a,b]	1.8±0.4
3	ZnO nanorods oral	2.7±0.4[a]	1.5±0.28	3.0±0.28

[a]Significant difference ($p<0.05$) compared to control;
[b]Significant difference ($p<0.05$) between i.v. and oral treatments.

nanorods showed more red pulp congestion than intravenously injected (Figs. 5a, 5b, 5c). The erythrocyte damage was evident from decreased RBC count due to ZnO nanorods treatment. Damaged RBCs are scavenged by the spleen which subsequently leads to the progression of toxic events in the spleen (Khan *et al.*, 1997) [37] resulting from nanorods treatment. Notably, iron released from damaged RBCs, deposited in the spleen may catalyze the free radical reactions results in the excess ROS generation which potentially react with biomolecules such as DNA, lipids particularly the fatty acid component of the membrane phospholipids and leads to membrane damage and cellular dysfunction. More red pulp congestion observed in the spleen of mice administered with ZnO nanorods orally might be due to the accumulation of nanorods that are directly distributed to the spleen and also are released from the damaged RBCs during destruction in the red pulp of the spleen. Congestion in the red pulp may lead to congestive splenomegaly.

Lung of mice treated intravenously with ZnO nanorods showed mild pulmonary vascular congestion whereas oral administered mice showed moderate pulmonary vascular congestion (image not shown). In general, 30-80 nm size nanoparticles are usually sequestered in the lung tissue [38]. The average crystal size of ZnO nanorods used in the present study is 50 nm. Hence the nanoparticles of such size may retain in the lungs led to vascular congestion, thereby pressure in the lungs blood vessels increases, fluid is pushed into the lungs results in shortening of breath.

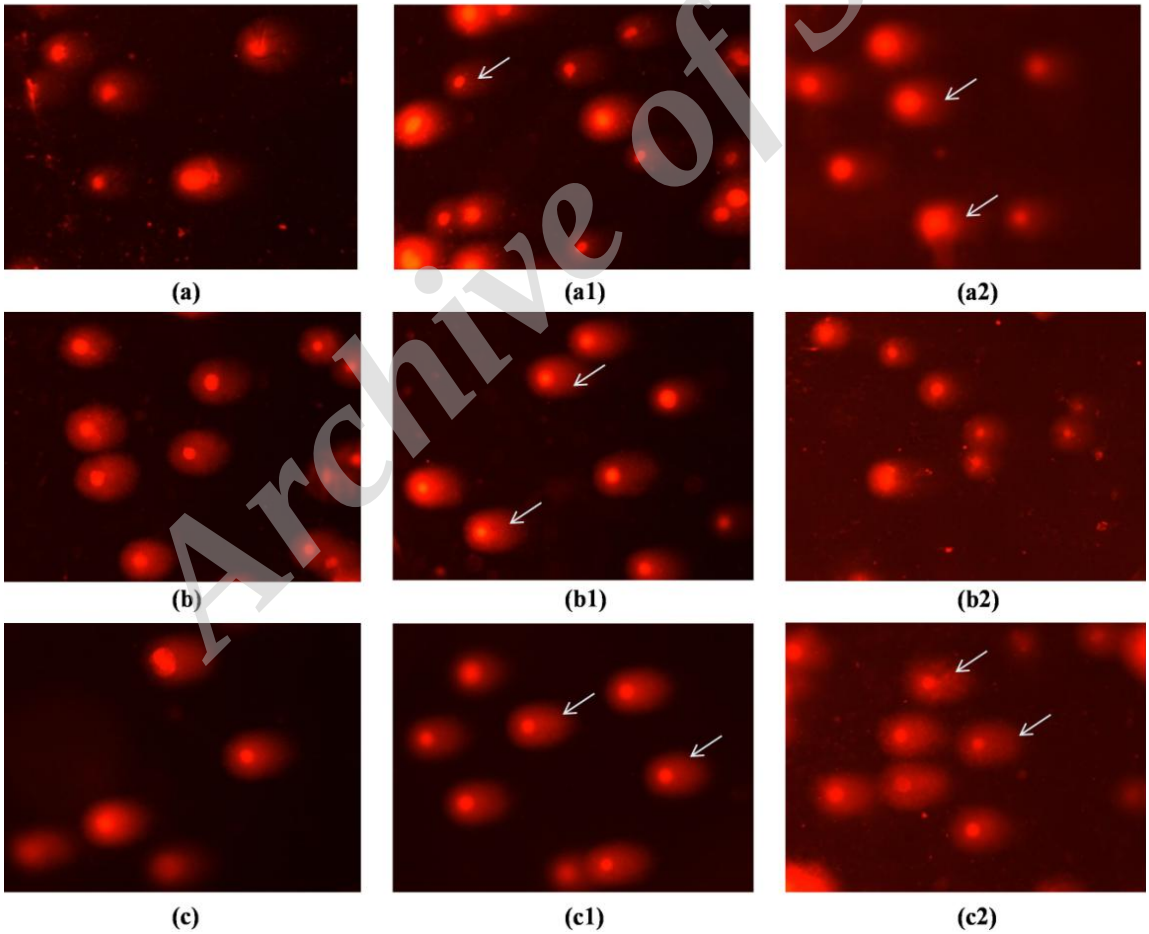

Fig. 3: Figures (a), (b) and (c); (a1), (b1) and (c1); (a2), (b2) and (c2) indicate comet images of liver, spleen and kidney tissues of untreated mice; mice treated intravenously with ZnO nanorods; mice treated orally with ZnO nanorods. DNA with comets is indicated by arrows in the figure.

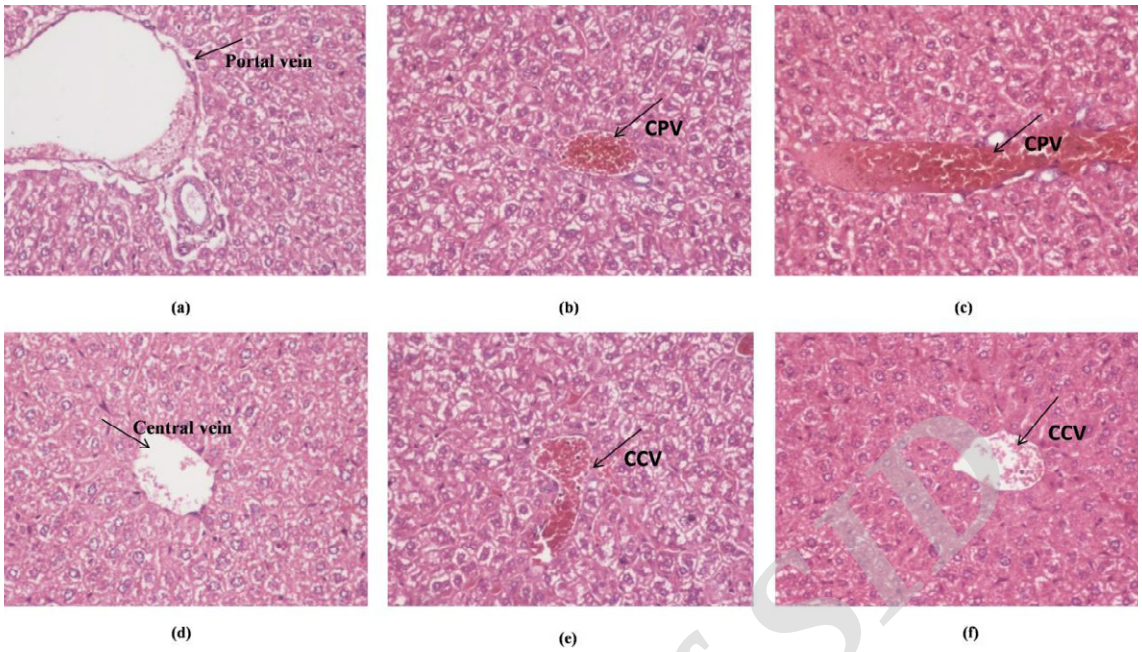

Fig. 4: Images (a) and (d) show portal and central veins of liver of untreated mice; (b) and (e) indicate congestion in portal and central veins of liver of mice treated intravenously with ZnO nanorods; (c) and (f) indicate congestion in portal and central veins of liver of mice treated orally with ZnO nanorods at 100x magnification. CCV-congestion in central vein; CPV-congestion in portal vein.

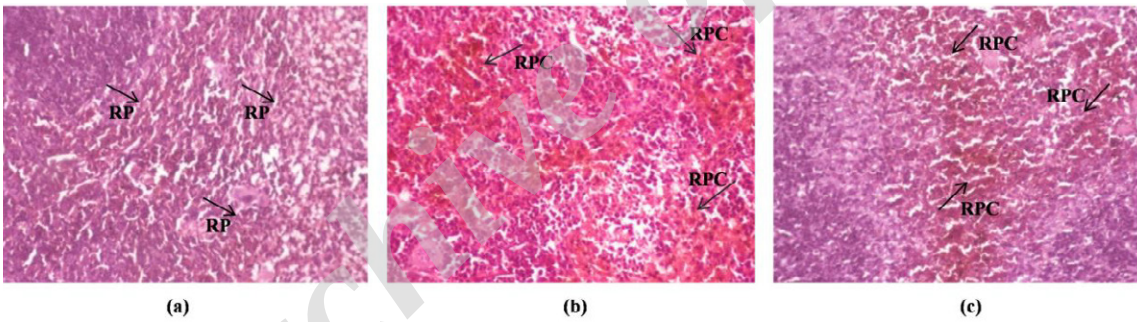

Fig. 5: Images (a), (b) and (c) indicate histology of mice spleen-untreated; intravenously treated; orally administered with ZnO nanorods at 100x magnification. RP-Red pulp; RPC-Red pulp congestion.

No histological changes were observed in kidneys of mice treated intravenously and orally with ZnO nanorods. The free radicals generated due to the slight increase in LPO in the kidney of oral treated mice in addition to the direct interaction of ZnO nanorods with DNA resulted in more DNA damage than kidney of intravenously treated mice. Even though ZnO nanorods induced significant DNA damage in the kidney of mice treated intravenously and orally, the unaltered levels of urea, creatinine observed in the present study indicated normal renal functions in mice treated with ZnO nanorods and also evident from normal histology of kidney. As observed by Burns *et al.*, 2009., [39] only smaller size nanoparticles (3-6 nm) are efficiently cleared by the kidney, whereas larger size particles (~30 nm) are retained in the liver. Elimination kinetics studied by Baek *et al.,* 2012 [25] have also shown that a small amount of ZnO nanoparticles were excreted via urine while the majority of nanoparticles excreted via feces, thus reduces their distribution to kidney, which may have resulted in the unaltered histology of the kidney observed in our study.

It is interesting to know that some researchers are focused on considerable attenuation of the harmful effects induced by metal oxide nanoparticles combination in vivo by treating

animals with a complex of innocuous bioactive substances, which may be theoretically expected to provide protective integral and/or metal-specific effect [40].

CONCLUSION

In summary, the present study shows that the acute exposure of ZnO nanorods investigated after 3 days of administration resulted in histological changes in liver, spleen of mice. Through evaluation of toxicity mediated by intravenous and oral administration routes, we found alterations in liver, spleen at the (i) tissue (focal venous congestion in portal and central veins of liver; congestion in red pulp of spleen), (ii) cellular (increased oxidative stress) and (iii) molecular levels (increased genotoxicity), but after intravenous route more profound effect was found with respect to decrease in hematological parameters such as RBC and platelet count. The reasons behind the differences in results obtained after oral and intravenous routes in the tissues are not known but securing the blood and tissue pharmacokinetic data would allow making links between the exposure of nanoparticles and the observed toxicity. Such preclinical studies may aid in understanding the interaction of nanoparticles with the biological system and the resultant biological effects and the mechanisms of toxicity. In addition to the studies described in this manuscript, studies on the potential of the ZnO nanorods to induce complement activation and inflammatory response, alterations in the expression profile of genes involved in oxidative stress and apoptosis in vivo may provide additional clues about the safety of such nanoparticles.

ACKNOWLEDGEMENTS

Authors are thankful to Dr. Tata N Rao, Centre for Nanomaterials, ARCI, Hyderabad for providing ZnO nanorods powder. Authors are grateful to Dr. R.P. Tripathi, ex-Director, Institute of Nuclear Medicine and Allied Sciences (INMAS), Delhi for necessary facilities provided for animal experiments.

CONFLICT OF INTEREST

The authors declare that there is no conflict of interests regarding the publication of this manuscript.

REFERENCES

[1] Barenholz Y., (2012), Doxil®--the first FDA-approved nano-drug: lessons learned. *J. Cont. Release.* 160: 117-134.

[2] Reddy L. H., Bazile D., (2014), Drug delivery design for intravenous route with integrated physicochemistry, pharmacokinetics and pharmacodynamics: Illustration with the case of taxane therapeutics. *Adv. Drug Deliv. Rev.* 71: 34-57.

[3] Majedi A., Davar F., Abbasi A. R., (2016), Metal-organic framework materials as nano photocatalyst. *Int. J. Nano Dimens.* 7: 1-14.

[4] Abdeen S., Geo S., Sukanya S., Praseetha P. K., Dhanya R. P., (2014), Biosynthesis of Silver nanoparticles from Actinomycetes for therapeutic applications. *Int. J. Nano Dimens.* 5: 155-162.

[5] Aula S., Lakkireddy S., Jamil K., Kapley A., Swamy A. V. N., Reddy L. H., (2015), Biophysical, biopharmaceutical and toxicological significance of biomedical nanoparticles. *RSC Adv.* 5: 47830-47836.

[6] Guo D., Wu C., Jiang H., Li Q., Wang X., Chen B., (2008), Synergistic cytotoxic effect of different sized ZnO nanoparticles and daunorubicin against leukemia cancer cells under UV irradiation. *J. Photochem. Photobiol. B.* 93: 119-126.

[7] Deng Y., Zhang H., (2013), The synergistic effect and mechanism of doxorubicin-ZnO nanocomplexes as a multimodal agent integrating diverse anticancer therapeutics. *Int. J. Nanomedic.* 8: 1835-1841.

[8] Yamaki K., Yoshino S., (2009), Comparison of inhibitory activities of zinc oxide ultrafine and fine particulates on IgE-induced mast cell activation. *Biometals.* 22: 1031–1040.

[9] Kim M. H., Seo J. H., Kim H. M., Jeong H. J., (2014), Zinc oxide nanoparticles, a novel candidate for the treatment of allergic inflammatory diseases. *Eur. J. Pharmacol*. 738: 31-39.

[10] Xiong H. M., Xu Y., Ren Q. G., Xia Y. Y., (2008), Stable aqueous ZnO@polymer core−shell nanoparticles with tunable photoluminescence and their application in cell imaging. *J. Am. Chem. Soc.* 130: 7522–7523.

[11] Ng S. M., Wong D. S. N., Phung J. H. C., Chua H. S., (2013), Integrated miniature fluorescent probe to leverage the sensing potential of ZnO quantum dots for the detection of copper (II) ions. *Talanta.* 116: 514–519.

[12] Sharma H., Singh A., Kaur N., Singh N., (2013), ZnO-based imine-linked coupled biocompatible chemosensor for nanomolar detection of Co^{2+}. *ACS Sustain. Chem. Eng.* 1: 1600–1608.

[13] Zhao D., Song H. J., Hao L. Y., Liu X., Zhang L. C., Lv Y., (2013), Luminescent ZnO quantum dots for sensitive and selective detection of dopamine. *Talanta.* 107: 133–139.

[14] Singh K., Chaudhary G. R., Singh S., Mehta S. K., (2014), Synthesis of highly luminescent water stable ZnO quantum dots as photoluminescent sensor for picric acid. *J. Lumin.* 154: 148–154.

[15] Zhang J., Zhao S. Q., Zhang K., Zhou J. Q., (2014), Cd-doped ZnO quantum dots-based immunoassay for the quantitative determination of bisphenol A. *Chemosphere.* 95: 105–110.

[16] Gu B. X., Xu C. X., Yang C., Liu S. Q., Wang M. L., (2011), ZnO quantum dot labeled immunosensor for carbohydrate antigen 19-9. Biosens. *Bioelectron.* 26: 2720–2723.

[17] Augustine R., Dominic E. A., Reju I., Kaimal B., Kalarikkal N., Thomas S., (2014), Investigation of angiogenesis and its mechanism using zinc oxide nanoparticle-loaded electrospun tissue engineering scaffolds. *RSC Adv.* 4: 51528-51536.

[18] Gojova A., Guo B., Kota R. S., Rutledge J. C., Kennedy I. M., Barakat A. I., (2007), Induction of inflammation in vascular endothelial cells by metal oxide nanoparticles: Effect of

particle composition. *Environ. Health Perspect.* 115: 403–409.

[19] Jeng H. A., Swanson J., (2006), Toxicity of metal oxide nanoparticles in mammalian cells. *J. Environ. Sci. Health A Tox. Hazard. Subst. Environ. Eng.* 41: 2699-2711.

[20] Yang H., Liu C., Yang D., Zhang H., Xi Z., (2009), Comparative study of cytotoxicity, oxidative stress and genotoxicity induced by four typical nanomaterials: the role of particle size, shape and composition. *J. Appl. Toxicol.* 29: 69–78.

[21] Osman I. F., Baumgartner A., Cemeli E., Fletcher J. N., Anderson D., (2010), Genotoxicity and cytotoxicity of zinc oxide and titanium dioxide in HEp-2 cells. *Nanomedicine (Lond.).* 5: 1193–1203.

[22] Sharma V., Singh P., Pandey A. K., Dhawan A., (2012), Induction of oxidative stress, DNA damage and apoptosis in mouse liver after sub-acute oral exposure to zinc oxide nanoparticles. *Mutat Res.* 745: 84-91.

[23] Cho W. S., Kang B. C., Lee J. K., Jeong J., Che J. H., Seok S. H., (2013), Comparative absorption, distribution, and excretion of titanium dioxide and zinc oxide nanoparticles after repeated oral administration. *Part. Fibre Toxicol.* 10: 9-16.

[24] Lee C. M., Jeong H. J., Yun K. N., Kim D. W., Sohn M. H., Lee J. K., Jeong J., Lim S. T., (2012), Optical imaging to trace near infrared fluorescent zinc oxide nanoparticles following oral exposure. *Int. J. Nanomedic.* 7: 3203-3209.

[25] Baek M., Chung H. E., Yu J., Lee J. A., Kim T. H, Oh J. M., Lee W. J., Paek S M., Lee J. K., Jeong J., Choy J. H., Choi S. J., (2012), Pharmacokinetics, tissue distribution, and excretion of zinc oxide nanoparticles. *Int. J. Nanomedicine.* 7: 3081-3097.

[26] Esmaeillou M., Moharamnejad M., Hsankhani R., Tehrani A. A., Maadi H., (2013), Toxicity of ZnO nanoparticles in healthy adult mice. *Environ. Toxicol. Pharmacol.* 35: 67-71.

[27] Choi J., Kim H., Kim P., Jo E., Kim H. M., Lee M. Y., Jin S. M., Park K., (2015), Toxicity of zinc oxide nanoparticles in rats treated by two different routes: single intravenous injection and single oral administration. *J. Toxicol Environ. Health A.* 78: 226-243.

[28] Cho W. S., Duffin R., Howie S. E., Scotton C. J., Wallace W. A., Macnee W., Bradley M., Megson I. L., Donaldson K., (2011), Progressive severe lung injury by zinc oxide nanoparticles; the role of Zn^{2+} dissolution inside lysosomes. *Part. Fibre. Toxicol.* 8: 27-34.

[29] http://ilocis.org/documents/chpt82e.htm.

[30] Aula S., Lakkireddy S., Swamy A. V. N., Kapley A., Jamil K., Tata N. R., Hembram K., (2014), Biological interactions in vitro of zinc oxide nanoparticles of different characteristics. *Mater. Res. Express.* 1: 035041-035046.

[31] Beutler E., Duron O., Kelly B. M., (1963), Improved method for the determination of blood glutathione. *J. Lab. Clin. Med.* 61: 882-888.

[32] Laughton M. J., Halliwell B., Evans P. J., Hoult J. R., (1989), Antioxidant and pro-oxidant actions of the plant phenolicsquercetin, gossypol and myricetin. Effects on lipid peroxidation, hydroxyl radical generation and bleomycin-dependent damage to DNA. *Biochem. Pharmacol.* 38: 2859-2865.

[33] Tice R. R., Agurell E., Anderson D., Burlinson B., Hartmann A., Kobayashi H., Miyamae Y., Rojas E., Ryu J. C., Sasaki Y. F., (2000), Single cell gel/comet assay: Guidelines for in vitro and in vivo genetic toxicology testing. *Environ. Mol. Mutagen.* 35: 206–221.

[34] Khaitan D., Chandna S., Arya M. B., Dwarakanath B. S., (2006), Differential mechanisms of radiosensitization by 2-deoxy-D-glucose in the monolayers and multicellular spheroids of a human glioma cell line. *Cancer Biol. Ther.* 5: 1142-1151.

[35] Countryman P. I., Heddle J. A., (1976), Production of micronuclei from chromosome aberrations in irradiated cultures of human lymphocytes. *Mutat. Res.* 41: 321–332.

[36] Alvarez A. M., Mukherjee D., (2011), Liver abnormalities in cardiac diseases and heart failure. *Int. J. Angiol.* 20: 135-142.

[37] Khan M. F., Boor P. J., Gu Y., Alcock N. W., Ansari G. A., (1997), Oxidative stress in the splenotoxicity of aniline. *Fundam. Appl. Toxicol.* 35: 22-30.

[38] Souris J. S., Lee C. H., Cheng S. H., Chen C. T., Yang C. S., Ho J. A., Mou C. Y., Lo L. W., (2010), Surface charge-mediated rapid hepatobiliary excretion of mesoporous silica nanoparticles. *Biomaterials.* 31: 5564-5574.

[39] Burns A. A., Vider J., Ow H., Herz E., Penate-Medina O., Baumgart M., Larson S. M., Wiesner U., Bradbury M., (2009), Fluorescent silica nanoparticles with efficient urinary excretion for nanomedicine. *Nano Lett.* 9: 442-448.

[40] Minigalieva I. A., Katsnelson B. A., Panov V. G., Privalova L. I., Varaksin A. N., Gurvich V. B., Sutunkova M. P., Shur V. Y., Shishkina E. V., Valamina I. E., Zubarev I. V., Makeyev O. H., Meshtcheryakova E. Y., Klinova S. V., (2017), In vivo toxicity of copper oxide, lead oxide and zinc oxide nanoparticles acting in different combinations and its attenuation with a complex of innocuous bio-protectors. *Toxicology.* 380: 72-93.